Acta Metallurgica, Vol. 25, pp. 395–406, Pergamon Press, 1977. Printed in Great Britain

THE DEVELOPMENT OF RECRYSTALLIZATION TEXTURES IN $(\bar{1}10)[001]$ AND $(\bar{1}10)[11\bar{2}]$ Ag SINGLE CRYSTALS AFTER A PLANE-STRAIN DEFORMATION OF 80.9%

S. HOEKSTRA* and J. W. H. G. SLAKHORST*†

Technical University Twente, Enschede, the Netherlands

and

J. HUBER‡

Technische Universität Clausthal, Clausthal-Zellerfeld, Bundesrepublik Deutschland

(*First received* 19 *May* 1976; *in revised form* 18 *August* 1976)

Abstract—After an 80.9% plane-strain deformation of Ag crystals with an initial orientation of $(\bar{1}10)[001]$ and $(\bar{1}10)[11\bar{2}]$ both orientations proved to be stable. The spread in orientation was no more than about 10° from the initial orientation. The new orientations resulting from the recrystallization process can reasonably be explained by a continuous array of twins. Both with X-ray techniques and by means of electron microscopy orientations within 5° of those of twins up to the fourth order have been observed. None of these twins possessed a 30–40° orientation relationship around a common $\langle 111 \rangle$ axis with the deformed matrix.

Résumé—On a trouvé que les orientation initiales $(\bar{1}10)[001]$ et $(\bar{1}10)[11\bar{2}]$ de monocristaux d'argent étaient stables après une déformation plane de 80.9%: La dispersion de l'orientation autour de sa valeur initiale ne dépassait pas une dizaine de degrés. On peut expliquer raisonnablement les nouvelles orientations provenant de la recristallisation par un réseau continu de macles. Les techniques de rayons X et la microscopie électronique ont permis d'observer des orientations différant de moins de 5 degrés de celles des macles jusqu'an 4 éme ordre. L'orientation, d'aucune de ces macles ne se de'duisait de celle de la matrice par une rotation de 30 à 40° autour d'umaxe $\langle 111 \rangle$ commun.

Zusammenfassung—Nach einer Verformung von Ag-Kristallen mit Anfangsorientierungen $(\bar{1}10)[001]$ und $(\bar{1}10)[112]$ in ebener Dehnung um 80.9% zeigten sich diese beiden Orientierungen stabil. Die Abweichungen der Orientierungen von der Ausgangsorientierung betrug nicht mehr als 10°. Die von einem Rekristallisationsprozess herrührenden neuen Orientierungen können mit einer kontinuierlichen Anordnung von Zwillingen zufriedenstellend erklärt werden. Sowohl mit Röntgenmethoden als auch mit der Elektronenmikroskopie wurden Orientierungen dieser Zwillinge innerhalb 5° bis zur vierten Ordnung beobachtet. Keiner dieser Zwillinge wies ein Orientierungsverhältnis von 30–40° um eine gemeinsame $\langle 111 \rangle$-Achse mit der verformten Matrix auf.

1. INTRODUCTION

Several investigators have reported the important role of twinning during the development of recrystallization textures in f.c.c. metals with a low stacking fault energy [1–4]. The recrystallization textures are assumed to be created due to either direct twinning of the deformed matrix [1–3] or due to twinning of nuclei formed by some mechanism, such as the inverse Rowland transformation (4). It is assumed that the final texture originates from the numerous twins formed by subsequent twinning after a selection of their growth capacity.

In the present investigations Ag single crystals have been deformed by means of a plane-strain compression test. The orientations of these specimens were $(\bar{1}10)[001]$ and $(\bar{1}10)[11\bar{2}]$. The $(\bar{1}10)[001]$ orientation is reported to be stable up to high amounts of deformation. According to Heye and Wassermann [5] and Verbraak and Slakhorst [6], it is not until 95% rolling reduction that this orientation rotates away toward $(\bar{1}10)[11\bar{2}] + (\bar{1}10)[112]$. The $(\bar{1}10)[11\bar{2}]$ orientation, however, remains stable throughout the deformation process. This implies that after deformations of 80.9% both orientations are still sufficiently sharp to present favorable conditions for oriented growth, as described by Parthasarathi and Beck [7]. Moreover the repeated twinning during recrystallization would provide growth nuclei covering a large range of orientations.

The orientations of the twins developing during the recrystallization process, and their orientation relationship with the deformed matrix has been studied both by X-ray techniques and the electron microscope. For that purpose the transversal plane of the specimen has been examined (i.e. the constrained plane), because this will offer a clearer picture of the structure of the deformed and recrystallizing specimens than observations on the compression plane.

2. THE EXPERIMENTAL PROCEDURE

Single crystals in the $(\bar{1}10)[001]$ and $(\bar{1}10)[11\bar{2}]$ orientations were machined carefully from an Ag

* Department of Mechanical Engineering, Materials Section.

† Dutch foundation for fundamental research of matter (FOM), Section Mt. VIII.

‡ Institut für Metallkunde und Metallphysik.

single crystal with a diameter of 25 mm and a purity of 99.999%. This Ag single crystal was obtained from Metals Research Ltd., Cambridge, G.B. The orientations of the specimens were determined by means of the X-ray Laue method. The dimensions of the machined specimens were 20.5 × 8.5 × 10.5 mm. The specimens were abraded on water-cooled sandpaper in a special specimen holder in order to retain the rectangular shape. Thus, the dimensions were reduced to 20.0 × 8.0 × 10.0 mm in order to remove all possible deformation caused by machining. The final dimensions of 20.0 × 8.0 × 9.996 + 0.002 mm were obtained by electrolytical polishing in a 5% KCN solution in distilled H_2O. An ultimate check proved that all orientations were within 3° of the desired one and that no broadening of the Laue spots due to residual strains could be observed.

The plane-strain compression tests were carried out at room temperature, while molycote was applied to the walls of the plane-strain apparatus, in order to reduce the frictional forces on the specimen. The strain rate amounted to 0.5–1 mm/min and after each reduction in thickness of 1 mm the specimen was rotated 180° around the transverse direction. After the completion of the deformation process the specimens were stored in liquid nitrogen.

From these specimens slices of 1 mm thickness were carefully sectioned parallel to the constrained plane (i.e. perpendicular to the transverse direction) by use of a very fine water-cooled hand saw. After sectioning the slices were abraded on water-cooled sandpaper and polished electrolytically in order to remove all the distorted material caused by sawing. In this way it was possible to avoid artificial nucleation during the annealing treatments, which were carried out in a thermostatically controlled oil-bath (±3°C), after which the amount of recrystallization was measured optically. Complete recrystallization curves were determined of each specimen at 150 and 175°C (Fig. 1).

{200} and {111} pole figures were recorded of the compression plane and the constrained (transversal) plane of the specimens. In the case of pole figures of the compression plane of the deformed specimens the influence of the surface texture was determined as well. Specimens in the deformed state and after very short times of annealing were studied electron microscopically. For this purpose the specimens were abraded mechanically (after the annealing treatment) until a thickness of 100 μm and then polished electrolytically in a "Struers Tenupol" in a solution of 5% KCN in distilled H_2O during 7.5 sec at 35V and at a minimum flow rate. The specimen polishing was finished by bath polishing between two point-cathodes in 5% KCN in H_2O at 4.5 V. The electron microscopy observations have been carried out on a Jeol 200A electron microscope, operated at 200 kV.

3. RESULTS

3.1 *The as deformed state*

3.1.1 *X-ray observations.* Figures 2 and 3 show the {111} pole figures of the constrained planes of the $(\bar{1}10)[001]$ and $(\bar{1}10)[11\bar{2}]$ specimens after a deformation of 80.9%. It can be seen that only a small spread around the initial orientation results from this deformation process. It has been observed that the $(\bar{1}10)[001]$ orientation does not start to split up in both stable end orientations $(\bar{1}10)[11\bar{2}]$ and $(\bar{1}10)[112]$ until 97.2%, and it is not until 99.5% that this splitting up is complete. At these high deformations also a large increase of the surface texture is observed. This surface layer has always been removed by polishing before recrystallizing the specimens.

As is to be expected [5, 6, 8] the $(\bar{1}10)[11\bar{2}]$ orientation proves to be stable throughout the deformation process. However, this specimen does not retain its rectangular shape, as can be seen from Fig. 4. Only the section between the two lines remains in contact

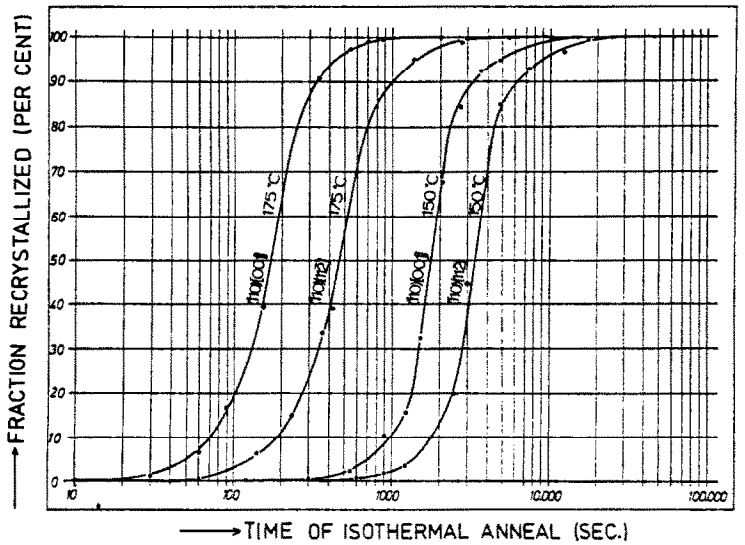

Fig. 1. Isothermal recrystallization curves of the Ag single crystals $(\bar{1}10)[001]$ and $(\bar{1}10)[11\bar{2}]$ plane-strained 80.9% and annealed at temperatures of 150 and 175°C.

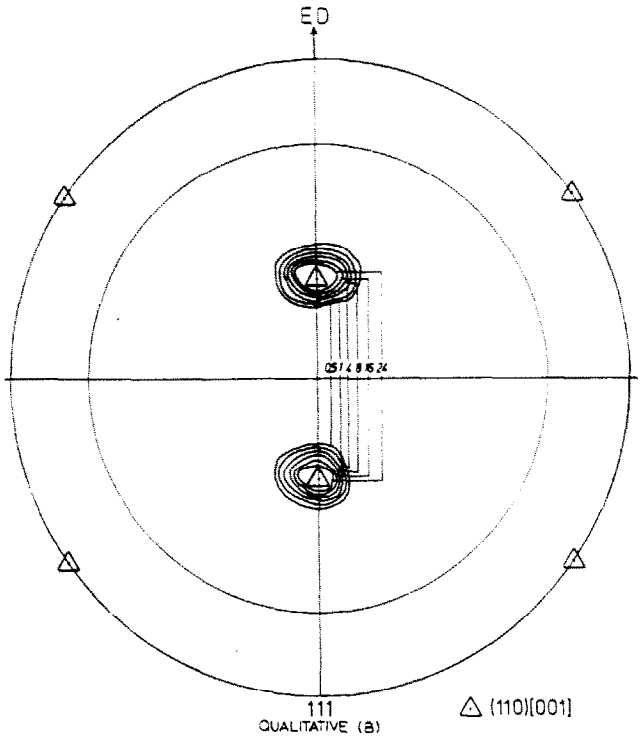

Fig. 2. {111} pole figure of the $(\bar{1}10)[001]$ specimen, plane-strained 80.9%. Plane of stereographic projection: ED–ND plane (constrained plane: ED = extension direction; ND = normal direction).

with the compression element of the plane-strain apparatus. Figure 3 represents the pole figure of this section. Figure 5 shows the {111} pole figure of the constrained plane of the section outside the two lines indicated in Fig. 4. From Fig. 5 the development of other texture components can easily be seen (compare Fig. 3). The most prominent one of these newly developed textures is the $(111)[\bar{1}\bar{1}2]$ twin component of the initial orientation $(111)[11\bar{2}]$ (with respect to the constrained plane and the extension direction ED). According to Chin *et al.* [9] a specimen with a $(\bar{1}10)[11\bar{2}]$ orientation (compression plane-extension

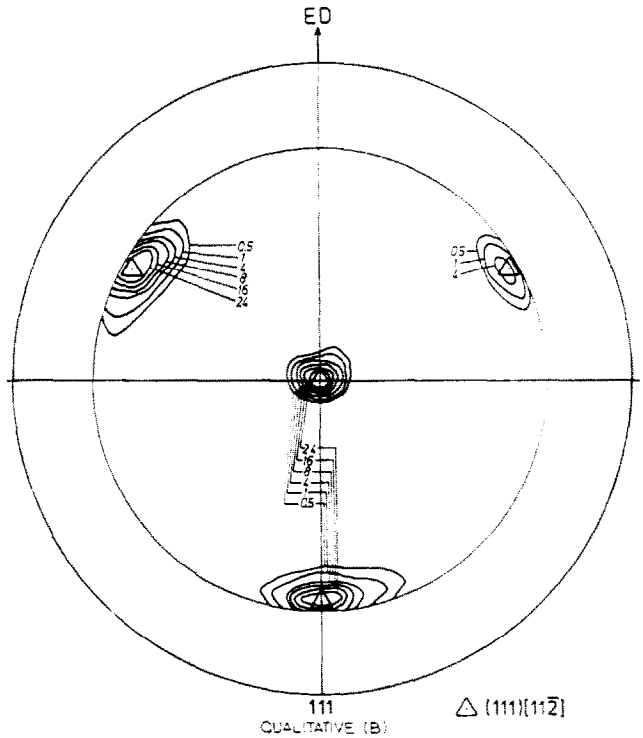

Fig. 3. {111} pole figure of the $(\bar{1}10)[11\bar{2}]$ specimen, plane-strained 80.9% of the region inside the two lines indicated in Fig. 4. Plane of stereographic projection: ED–ND plane (constrained plane).

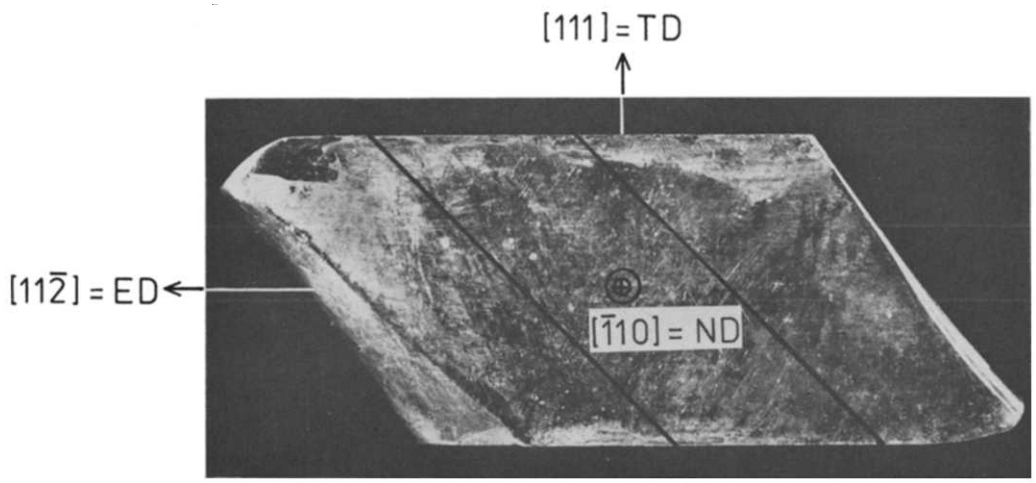

Fig. 4. Photograph of the ($\bar{1}$10)[11$\bar{2}$] specimen, plane-strained 58.6%. The viewing plane is the compression plane (ED–TD plane; TD = transverse direction).

direction) is expected to lose its rectangular shape when it is deformed by free rolling or plane-strain deformation, due to the assymetrical arrangement of the slip systems. The twin component originates from mechanical twinning on the constrained plane due to frictional forces from the specimen with the walls of the plane-strain apparatus (shear texture). This can be concluded from the fact that free-rolling of this specimen produces an even more oblique specimen, however, without the twin components which can be detected on the sides of the obtuse angles.

3.1.2 *Electron microscopy observations.* The constrained plane of both orientations has been examined in the electron microscope at a reduction in thickness of 80.9%. This implicates that both specimens still had their initial orientation (compare Figs. 2 and 3). In the case of the specimen with initial orientation ($\bar{1}$10)[11$\bar{2}$] foils were prepared from the section inside the two lines indicated in Fig. 4. Both specimens have a very similar cell-like structure with a small spread in orientation as can be seen from Fig. 6.

3.2 *The recrystallized state*

3.2.1 *Electron microscopy observations. The specimen with the initial orientation* ($\bar{1}$10)[001]. The specimens studied with the electron microscope were annealed during 5 sec at 175°C and during 2, 3, 4 and 5 min at 150°C. These times were chosen in order to investigate the very first beginning of the recrystallization process (compare Fig. 1). In the first stage

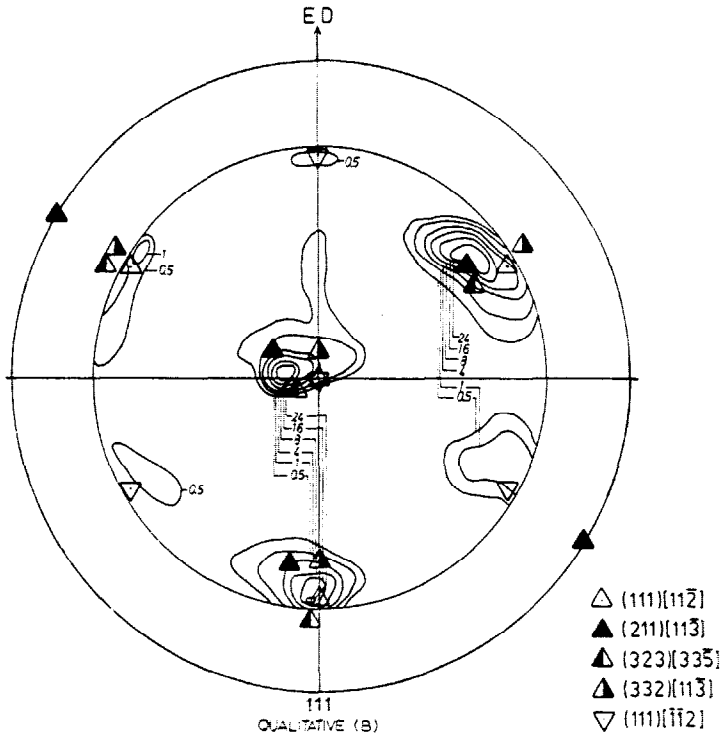

Fig. 5. {111}pole figure of the ($\bar{1}$10)[11$\bar{2}$] specimen, plane-strained 80.9%, of the region outside the two lines indicated in Fig. 4. Plane of stereographic projection: ED–ND plane (constrained plane).

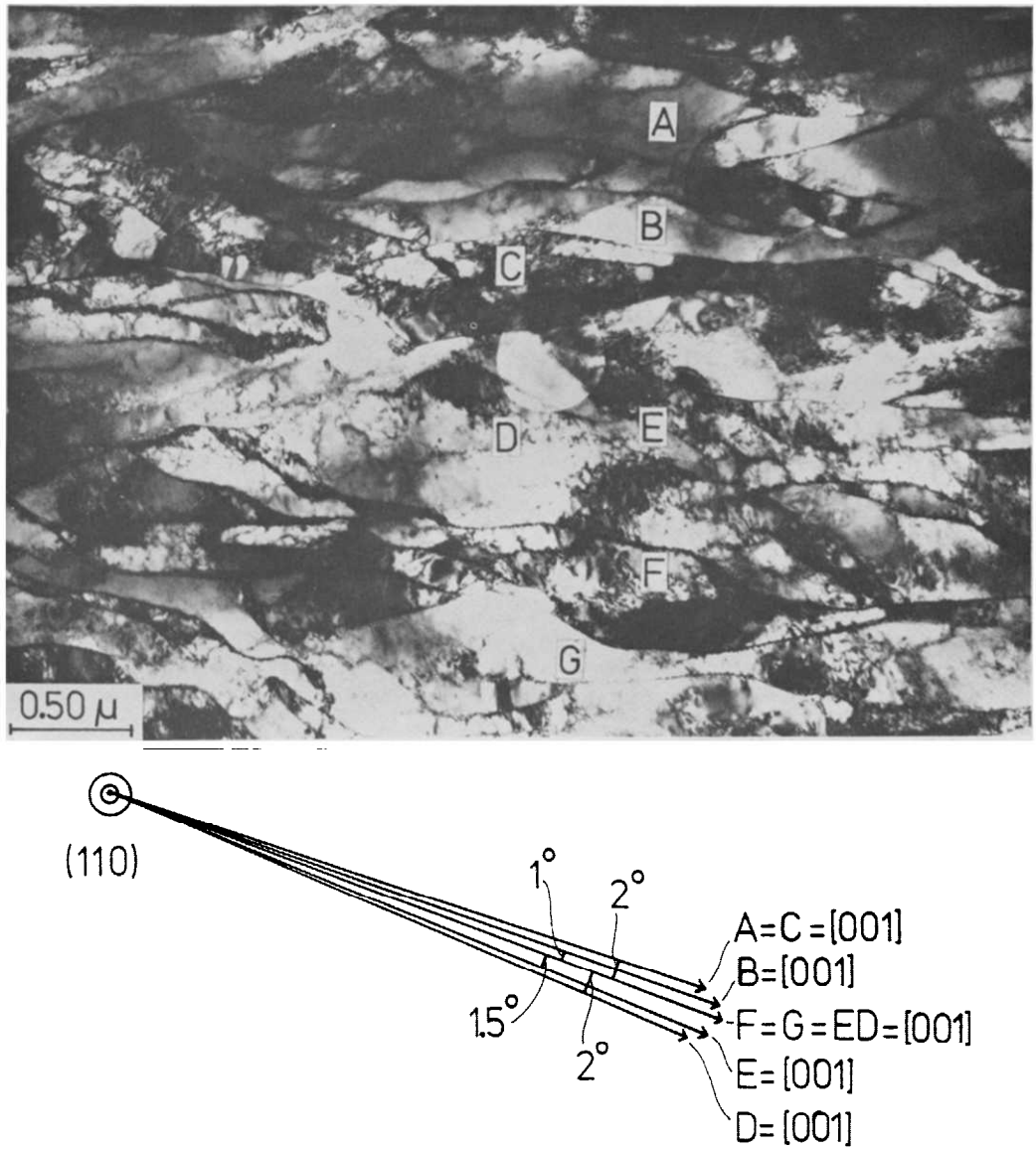

Fig. 6. Electron microscope observation of the $(\bar{1}10)[001]$ specimen, plane-strained 80.9% showing a very homogeneous orientation distribution. The viewing plane is the constrained plane (i.e. (110) = ED–ND plane).

of the recrystallization process growth of deformation subgrains is observed (Fig. 7). This can be attributed to a "micro bulging" mechanism as proposed by Bailey & Hirsch (10). The further development of the recrystallization is characterized by repeated twinning. The new grains all have a twin relationship of various order (up to the fourth) with the deformed matrix (Fig. 8). Table 1 summarizes the orientations observed in recrystallizing grains. The second row of the table presents the calculated twin orientations. It can easily be seen that there is a reasonable agreement between the observed and the calculated values. The largest angular discrepancy exists between the fourth order twin $(23\ 7\ 11\bar{2})[28\ \overline{76}\ \bar{1}]$ and the observed orientation $(001)[1\bar{2}0]$ (this is 12°). However, it should be noted that due to the limited transmittable specimen thickness no Kikuchi lines were observed in these specimens. This leads to an accuracy for the orientation determinations of 5°. Furthermore, it is known that cube oriented diffraction patterns are very stable against tilting in the electron microscope, because the nearest detectable orientation is $\{510\}$, which is 11° away from the cube orientation. Thus, the accuracy for cube oriented patterns is even less. Table 2 shows the sequence of twin families. In combination with Table I, it can be seen that most twins can be explained by subsequent twinning. The fact that not all of the twins can be described in this way probably has to be attributed to the limited number of individual orientation determinations. A more complete survey of the orientations present in the recrystallized state would almost certainly fill up this gap.

The specimens with the initial orientation $(\bar{1}10)[11\bar{2}]$. Most of these specimens were heat treated during 4 min at 150°C, whereas only the section inside the

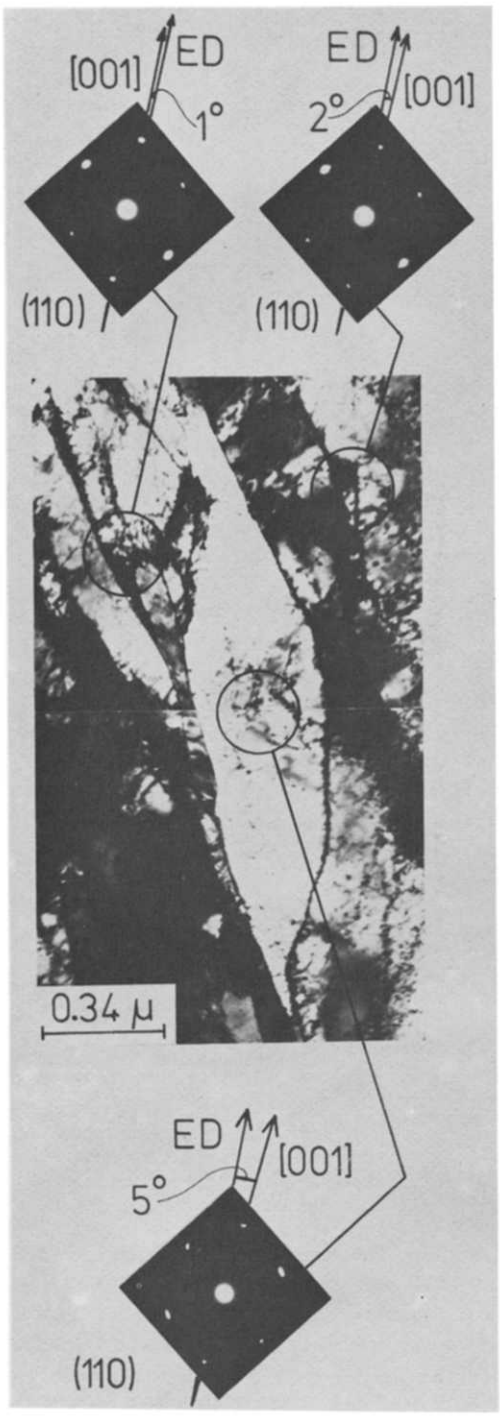

Fig. 7. Electron microscope observations of the $(\bar{1}10)[001]$ specimen, plane-strained 80.9% and annealed 3 min at 150°C. The viewing plane is the constrained plane (i.e. (110) = ED–ND plane).

two lines indicated in Fig. 4 was used for specimen preparation. The results from these experiments largely confirm those described in the previous section. The dominating role of twinning is as clear from this specimen as it is from the $(\bar{1}10)[001]$ specimen. Figure 9 presents an excellent example by showing a recrystallized grain of approximately 7 μm square, within a fully deformed matrix, having an orientation $(105)[\bar{5}\bar{5}1]$, which can be interpreted as the $(115)[\bar{5}\bar{5}2]$ orientation of the first twin of the deformed matrix. This is also confirmed by the shape of this grain. The fact, however, that the observed (105) orientation is 11° away from the ideal (115) orientation has to be attributed to the tilting of the specimen. Furthermore also third and fourth order twins can be observed in Fig. 9. All twins observed are tabulated in Table 3, whereas Table 4 again gives the relation between the various twins.

3.2.2 *The X-ray observations.* Annealing treatments, chosen from the recrystallization data of Fig. 1, were carried out to study the development of the recrystallization texture. The textures obtained after complete recrystallization are shown in Figs. 10 and 11. These pole figures correspond again with the constrained plane, thus the initial orientation $(\bar{1}10)[001]$ is seen as $(110)[001]$ and $(\bar{1}10)[11\bar{2}]$ as $(111)[11\bar{2}]$. It is easily seen that these pole figures contain a very large amount of orientations, which can be covered excellently by a number of calculated twin orientations of fourth order. None of these orientations, however, possess a 30° orientation relationship around a common ⟨111⟩ pole with the deformed matrix, as is indicated by the traces connecting the various ⟨111⟩ poles after the rotation of 30°. There is, however, another feature which requires some attention. This is the fact that the twins observed in the pole figures were not detected by means of the electron microscope and vice versa. There are two factors which could explain this fact. In the first place all electron microscopy observations were carried out at times far shorter than those leading to complete recrystallization. Thus only those twins formed during the very first beginninng of the recrystallization process are observed. This also explains the fact that only fourth order twins are present in the pole figures, for all new orientations are produced by subsequent twinning. Secondly the orientation distribution obtained even from several hundreds of diffraction patterns in a small area is not comparable to the orientation distribution obtained from the larger area surveid by pole figure determination [11].

4. DISCUSSION

Although the accuracy of the electron microscopy orientation determinations is not better than 5° and in the case of the cube diffraction patterns even less, the agreement between the observed orientations and the calculated twin orientations (Tables 1 and 3)—which is usually better than the accuracy mentioned and which is unfavourably affected by the spread in the initial orientation—indicate the fact that the course of the recrystallization process is characterized by repeated twinning. This is confirmed by the twin shaped grains present in the bright field images, as well as by the X-ray pole figure orientation determinations. The role of twinning seems to be that dominant that it is doubtful whether a stable end orientation is present. Elongation of the annealing

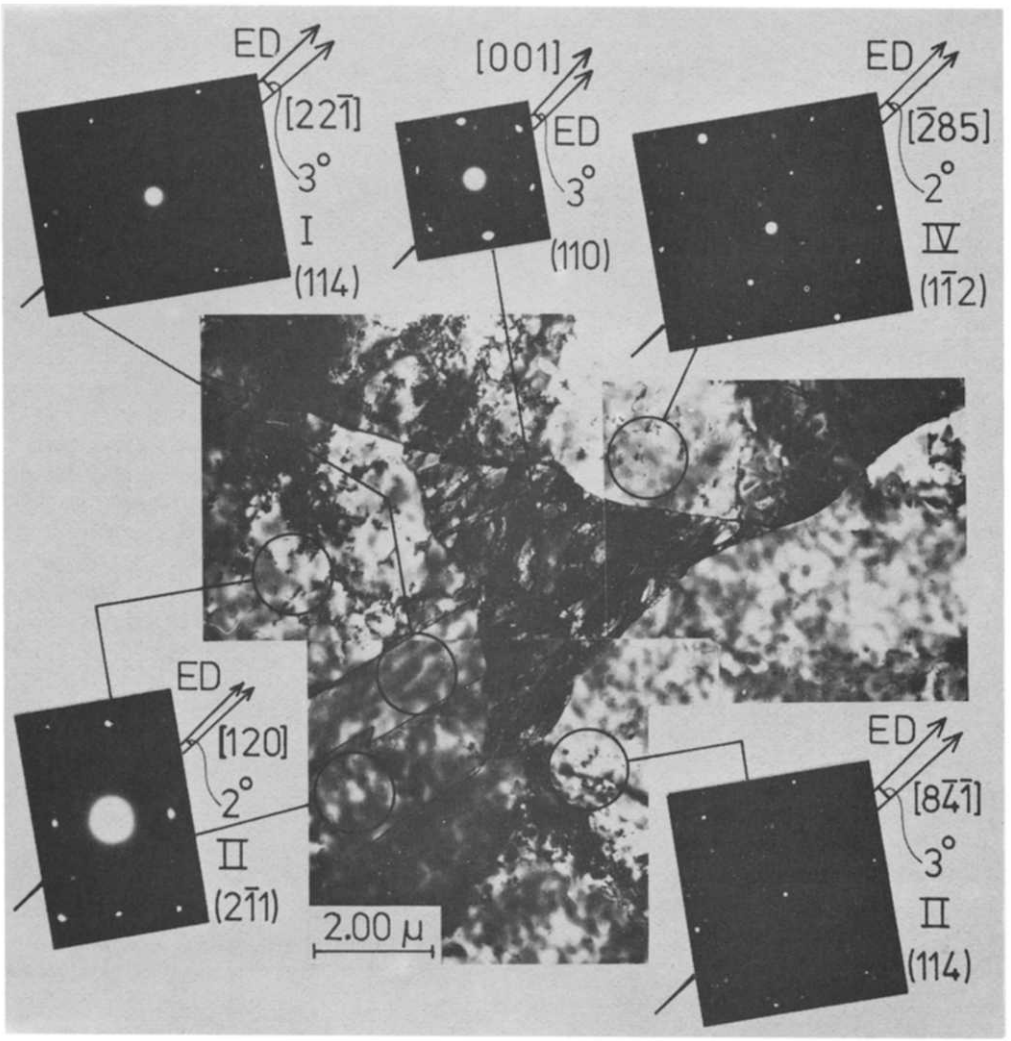

Fig. 8. Electron microscope observations of the (110)[001] specimen, plane-strained 80.9% and annealed 3 min at 150°C. The viewing plane is the constrained plane (i.e. (110) = ED–ND plane in the deformed structure). I = first order twin; II = second order twin; IV = fourth order twin.

time produces further twinning, both to higher order twins and to lower order twins (due to back-twinning).

Earlier investigations [1, 2, 4] have described the role of growth selection among the twins. This selection is based on the theories developed by Beck [12], which is strongly supported by Lücke *et al.* [13]. The theory states that during recrystallization those orientations present in the deformed matrix are supposed to grow out which have a 30–40° orientation relation-

Table 1. Observed and calculated twin orientations of the ($\bar{1}$10)[001] specimen, related to the constrained plane with initial orientation (110)[001]

	Observed orientation	Corresponds to calculated twin orientation
First order twins	(110)[2$\bar{2}$1]	(110)[2$\bar{2}$1]
	(114)[22$\bar{1}$]	(114)[22$\bar{1}$]
Second order twins	(114)[8$\bar{4}\bar{1}$]	(114)[8$\bar{4}\bar{1}$]
	(2$\bar{1}$1)[120]	(11 $\bar{5}$ 4)[48$\bar{1}$]
	(110)[44$\bar{7}$]	(110)[44$\bar{7}$]
Third order twins	(112)[$\bar{3}$5$\bar{1}$]	(5 4 11)[$\bar{1}\bar{4}$ 23 $\bar{2}$]
	(114)[$\bar{2}\bar{6}$ $\bar{2}$ 7]	(114)[$\bar{2}\bar{6}$ $\bar{2}$ 7]
Fourth order twins	(1$\bar{1}$2)[$\bar{2}$85]	(53 $\bar{4}\bar{3}$ 92)[$\bar{1}\bar{6}$ 68 41]
	(112)[$\bar{1}$11]	(4 5 11)[$\bar{5}\bar{5}$ $\bar{4}\bar{4}$ 40]
	(130)[3$\bar{1}$3]	(35 109 4)[56 $\bar{2}\bar{0}$ 55]
	(001)[1$\bar{2}$0]	(23 7 112)[28 $\bar{7}\bar{6}$ $\bar{1}$]

Table 2. Sequence of twin families of the $(\bar{1}10)[001]$ specimen. IO = initial orientation of the constrained plane: I = first order twin; II = second order twin; III = third order twin: IV = fourth order twin

IO	$(110)[001]$		
I	$(110)[2\bar{2}1]$		$(114)[22\bar{1}]$
II	$(110)[4\bar{4}7]$	$(114)[8\bar{4}1]$	$(11\bar{5}4)[48\bar{1}]$
III	$(114)[\bar{2}6\,\bar{2}\,7]$	$(5\,4\,11)[\bar{1}4\,23\,\bar{3}]$	
IV	$(4\,5\,11)[\bar{3}5\,\bar{4}4\,40]$		

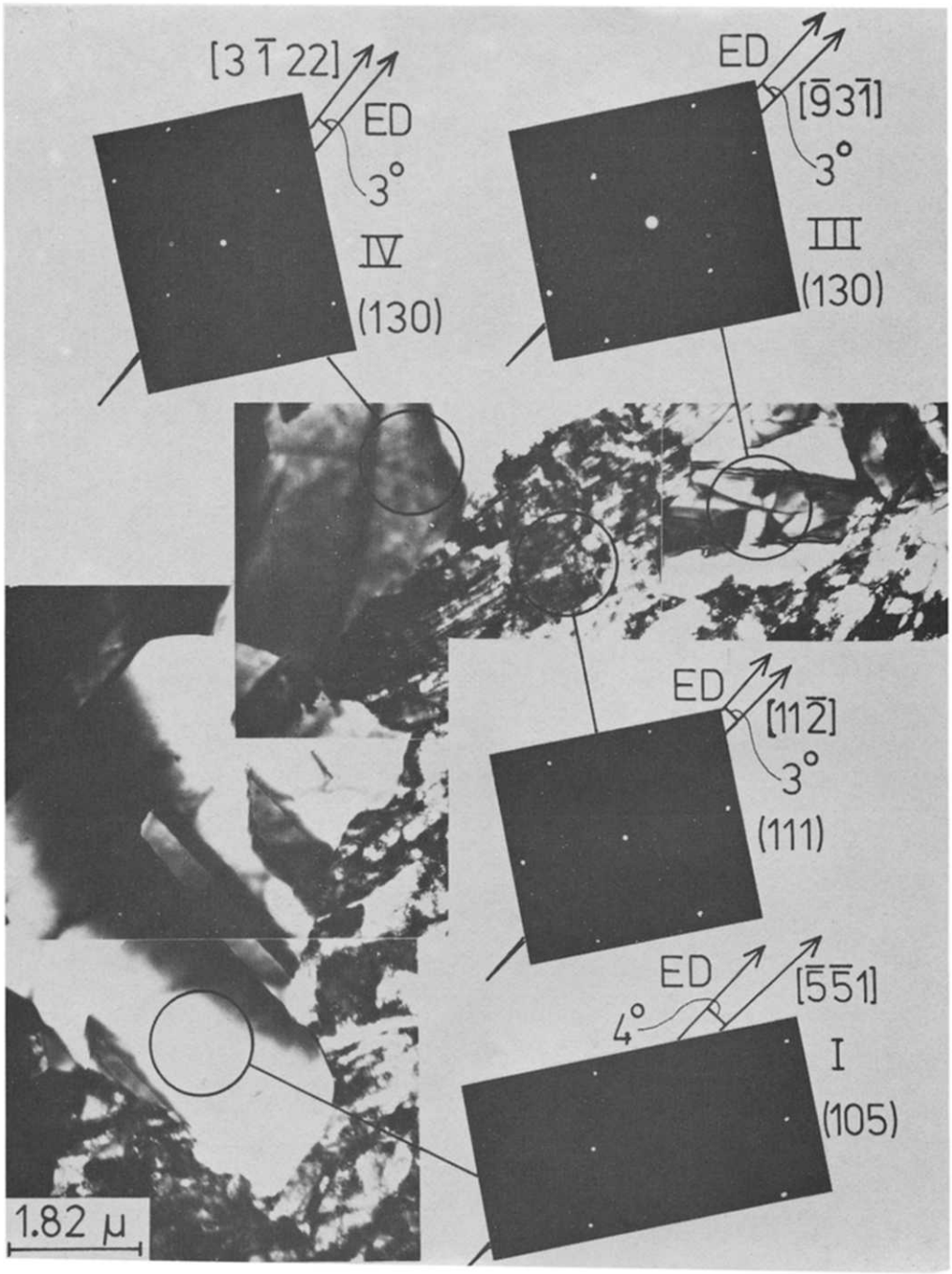

Fig. 9. Electron microscope observations of the $(\bar{1}10)[11\bar{2}]$ specimen. plane-strained 80.9% and annealed 4 min at 150°C. The viewing plane is the constrained plane (i.e. (111) = ED–ND plane in the deformed structure). I = first order twin; III = third order twin; IV = fourth order twin.

Table 3. Observed and calculated twin orientations of the $(\bar{1}10)[11\bar{2}]$ specimen, related to the constrained plane with initial orientation $(111)[11\bar{2}]$

	Observed orientation	Corresponds to calculated twin orientation
First order twins	$(105)[\bar{5}\bar{5}1]$	$(115)[\bar{3}\bar{3}2]$
	$(611)[\bar{1}7\bar{1}]$	$(511)[\bar{1}\bar{7}2]$
Second order twins	$(110)[001]$	$(11\,11\,\bar{1})[1\,1\,22]$
	$(110)[\bar{3}3\bar{2}]$	$(11\,11\,\bar{1})[\bar{1}4\,13\,\bar{1}1]$
	$(011)[1\bar{1}1]$	$(\bar{1}\,11\,11)[11\,\bar{1}3\,14]$
Third order twins	$(130)[\bar{9}3\bar{1}]$	$(17\,43\,\bar{7})[\bar{6}1\,22\,\bar{1}3]$
	$(110)[\bar{3}34]$	$(35\,31\,1)[\bar{3}4\,37\,43]$
	$(011)[5\bar{1}1]$	$(\bar{1}\,35\,31)[65\,\bar{7}\,10]$
	$(110)[221]$	$(31\,35\,1)[\bar{4}7\,41\,22]$
Fourth order twins	$(130)[3\,\bar{1}\,22]$	$(49\,131\,\bar{1}1)[46\,\bar{1}\,193]$
	$(001)[\bar{4}30]$	$(19\,1\,139)[\bar{1}46\,133\,19]$
	$(001)[\bar{2}10]$	$(17\,25\,137)[\bar{1}85\,71\,10]$
	$(001)[\bar{5}40]$	$(19\,1\,139)[\bar{1}46\,133\,19]$
	$(001)[\bar{1}10]$	$(1\,19\,139)[\bar{1}33\,146\,\bar{1}9]$
	$(001)[\bar{1}20]$	$(25\,17\,137)[\bar{7}1\,185\,\bar{1}0]$

Table 4. Sequence of twin families of the $(\bar{1}10)[11\bar{2}]$ specimen. IO = initial orientation of the constrained plane; I = first order twin; II = second order twin; III = third order twin

IO	$(111)[11\bar{2}]$	
I	$(115)[\bar{3}\bar{3}2]$	$(511)[\bar{1}\bar{7}2]$
II	$(11\,11\,\bar{1})[1\,1\,22]$	$(11\,11\,\bar{1})[\bar{1}4\,13\,\bar{1}1]$ $(\bar{1}\,11\,11)[11\,\bar{1}3\,14]$
III	$(31\,35\,1)[\bar{4}7\,41\,22]$	$(35\,31\,1)[\bar{3}4\,37\,43] + (\bar{1}\,35\,31)[65\,\bar{7}\,10]$

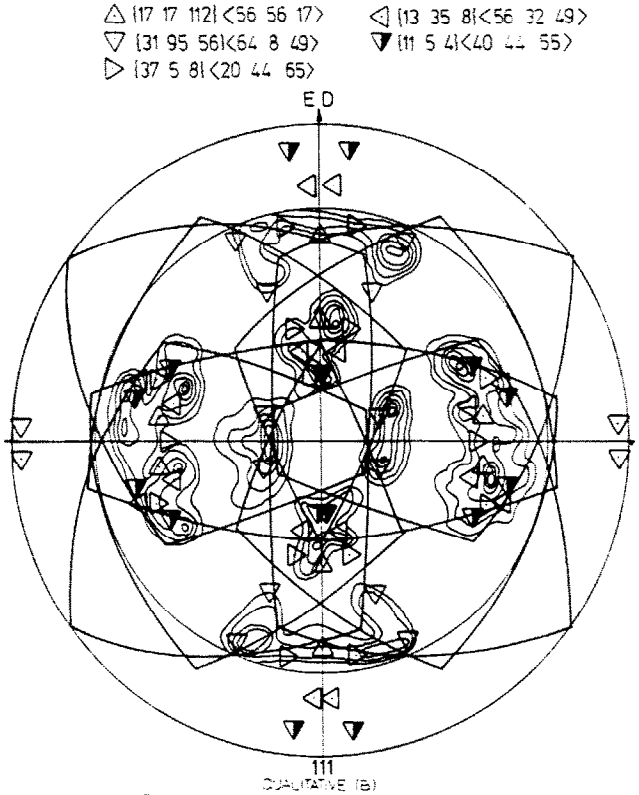

Fig. 10 {111} pole figure of the $(\bar{1}10)[001]$ specimen, plane-strained 80.9% and annealed to complete recrystallization. Plane of stereographic projection: ED–ND plane (constrained plane).

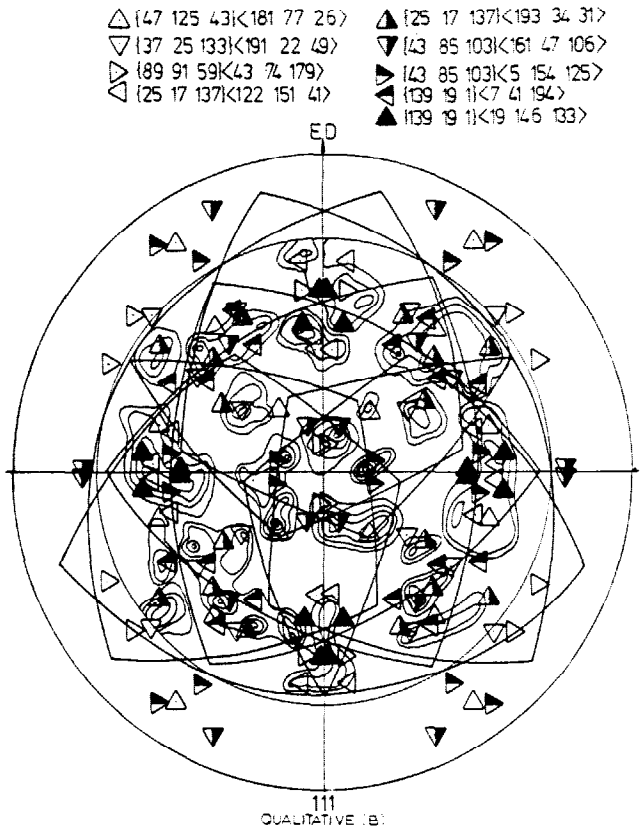

Fig. 11. {111} pole figure of the $(\bar{1}10)[11\bar{2}]$ specimen, plane-strained 80.9% and annealed to complete recrystallization. Plane of stereographic projection: ED–ND plane (constrained plane).

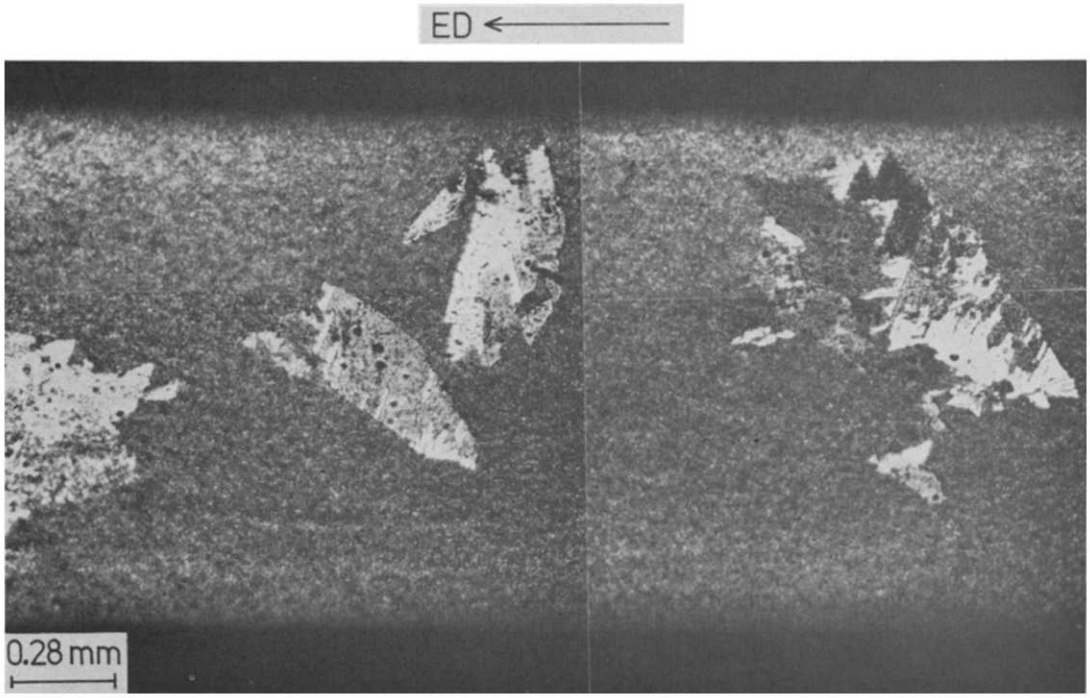

Fig. 12. Optical micrograph of the $(\bar{1}10)[001]$ specimen, plane-strained 80.9% and annealed 25 min at 150°C. The viewing plane is the constrained plane (ED–ND plane). Fraction recrystallized: 32%.

ship around a common ⟨111⟩ axis with the deformed matrix. In the specimen with a (110) constrained plane and [001] extension direction (the $(\bar{1}10)[001]$ specimen) crystals with {148} or {4 7 11} constrained plane and corresponding ⟨843⟩ and ⟨384⟩ extension direction would have this required orientation relationship. In the specimen with a (111) constrained plane and $[11\bar{2}]$ extension direction (the $(\bar{1}10)[11\bar{2}]$ specimen) the favourable orientations are: {111}⟨156⟩, {148}⟨452⟩, {148}⟨474⟩ and {148}⟨12 1 1⟩ (constrained plane-extension direction). Even if the accuracy of 5° is taken into account, the orientations observed are rather remote from these orientations. Trace analysis, indicated in Figs. 10 and 11, confirms this conclusion.

The narrow spread in orientation of the deformed matrix (compare Figs. 2, 3 and 6) will lead to a lack of nucleation sites and recrystallization will proceed very reluctantly [14]. This is shown in Fig. 12, where only a few nuclei are visible in the deformed matrix in the first stages of recrystallization. These nuclei will grow until their mutual impingement completes the recrystallization process without the formation of new nuclei, which results in a coarse grained structure. An example of a nucleus growing out to a considerable size is given in Fig. 13, showing a fourth order twin (as indicated by the cube etch pits). It is relevant to note that the $(\bar{1}10)[001]$ specimen recrystallizes faster than the $(\bar{1}10)[11\bar{2}]$ specimen (compare Fig. 1). This can be attributed to the fact that during the deformation of the crystals more slip systems are active in the $(\bar{1}10)[001]$ specimen (four slip systems) than in the $(\bar{1}10)[11\bar{2}]$ specimen (two slip systems).

Because of the narrow spread in orientation in the deformed matrix the required nuclei for oriented growth are missing in the very first stage of the recrystallization process. After the creation of the first twins, however, growth selection should distinguish between

Fig. 13. Optical micrograph of the $(\bar{1}10)[001]$ specimen, plane-strained 80.9% and annealed 60 min at 150°C. The viewing plane is the constrained plane (ED–ND plane). Fraction recrystallized: 93%.

those twins. However, this does not seem to happen.

It still should be explained how the twins which are observed are nucleated and why they grow out.

The nucleation of the twins can be understood by growth accidents as described by Gleiter [15]. These growth accidents may be favoured by dislocation reactions in a way similar to those proposed by Maddin *et al.* [16], although twinning was assumed to occur on the previous slip planes only. In our case twins were observed on all four {111} planes. Dislocation reactions similar to those described by Ogawa and Maddin [17] for the nucleation of mechnical twins in b.c.c. metals, however, may favour nucleation on other {111} planes as well [18]. The growth of the twins can be explained by assuming that once by accident a twin nucleus is created, this nucleus is capable of growth by subsequent deposition of {111} layers in the twin sequence [19]. This deposition is favoured by the incorporation of dislocations in the boundary as is described by Verbraak [20] and Sleeswijk and Verbraak [21]. A change of specific {111} planes on which the new layers are deposited produces twins of higher order. The boundaries created by this change are non-coherent and will therefore be mobile on further annealing. It is essential to notice that this process does not lead to a 30–40° orientation relationship between the growing grain and the matrix around a common ⟨111⟩ axis. This relationship apparently is not an essential prerequisite for growth of a nucleus in a deformed matrix with such a sharp texture as produced in the single crystals described in this investigation.

5. SUMMARY AND CONCLUSIONS

After an 80.9% plane-strain deformation of Ag crystals with an initial orientation of $(\bar{1}10)[001]$ and $(\bar{1}10)[11\bar{2}]$ both orientations proved to be stable. The spread in orientation was no more than about 10° from the initial orientation. In spite of this homogeneity in orientation the specimens readily recrystallized. The new orientations resulting from the recrystallization process can reasonably be explained by a continuous array of twins. Both with X-ray techniques and by means of electron microscopy orientations within 5° of those of twins up to the fourth order have been observed. None of these twins possessed a 30–40° orientation relationship around a common ⟨111⟩ axis with the deformed matrix. The twins are supposed to be created by the growth accident theory, proposed by Gleiter [15, 19].

Acknowledgements—The authors wish to thank Prof. Dr.-Ing. J. Grewen, Prof.dr.ir. C. A. Verbraak and Prof. Dr. G. Wassermann for the possibility that this work could be done at the "Institut für Metallkunde und Metallphysik der Technische Universität Clausthal" in Clausthal–Zellerfeld (BRD) and for the many helpful discussions with them in the course of the investigation. Further grateful thanks are due to all members of the institution in Clausthal–Zellerfeld who have contributed to this work. One of the authors (S.H.) gratefully acknowledges the financial support of the STIOMAK foundation. The work of J.W.G.H.S. is part of the research programme of the research group FOM-TNO of the "Stichting voor fundamenteel onderzoek der materie" (Foundation for fundamental research of matter—F.O.M.) and was made possible by financial support from the "Nederlandse organisatie voor zuiver wetenschappelijk onderzoek" (Dutch Organisation for pure research—Z.W.O).

REFERENCES

1. B. F. Peters, *Met. Trans.* **4**, 757 (1973).
2. B. F. Peters and D. C. Reid, *Met. Trans.* **4**, 2851 (1973).
3. S. G. Khayutin, *Phys. Met. Metallogr.* **29**, 211 (1970).
4. J. W. H. G. Slakhorst, *Acta Met.* **23**, 301 (1975).
5. W. Heye and G. Wassermann, *Z. Metallk.* **59**, 617 (1968).
6. C. A. Verbraak and J. W. H. G. Slakforst, *Scripta Met.* **8**, 217 (1974).
7. M. N. Parthasarathi and P. A. Beck, *Trans. AIME* **221**, 831 (1961).
8. I. L. Dillamore, E. Butler and D. Green, *Met. Sci. J.* **2**, 161 (1968).
9. G. Y. Chin, R. N. Thurston and E. A. Nesbitt, *Trans. AIME* **236**, 69 (1966).
10. J. E. Bailey and P. H. Hirsch, *Proc. R. Soc.* (A) **267**, 11 (1962).
11. F. Haessner, U. Jakubowski and M. Wilkens, *Phys. Status Solidi* **7**, 701 (1964).
12. P. A. Beck, *Z. Metallk.* **52**, 13 (1961).
13. K. Lücke, *Can. Met. Quart.* **13**, 261 (1974).
14. W. G. Burgers and P. C. Louwerse, *Z. Phys.* **61**, 605 (1931).
15. H. Gleiter, *Acta Met.* **17**, 1421 (1969).
16. R. Maddin, C. H. Mathewson and W. R. Hibbard, *Met. Trans.* **185**, 655 (1949).
17. K. Ogawa and R. Maddin, *Acta Met.* **12**, 713 (1964).
18. J. Friedel, *Dislocations*, p. 182. Pergamon Press, Oxford (1967).
19. H. Gleiter, *Acta Met.* **17**, 565 (1969).
20. C. A. Verbraak, *Z. Metallk.* **55**, 723 (1964).
21. A. W. Sleeswijk and C. A. Verbraak, *Acta Met.* **9**, 917 (1961).